PCCP

Water Plays a Dynamical Role in a Hydrogen-Bonded, Hexameric Supramolecular Assembly

Journal:	*Physical Chemistry Chemical Physics*
Manuscript ID	CP-ART-12-2019-006874.R1
Article Type:	Paper
Date Submitted by the Author:	11-Feb-2020
Complete List of Authors:	Katiyar, Ankita; University of Kansas, Department of Chemistry Freire Sovierzoski, Julia; University of Kansas, Department of Chemistry Calio, Paul; University of Kansas, Department of Chemistry Vartia, Anthony; University of Kansas, Department of Chemistry Thompson, Ward; University of Kansas, Department of Chemistry

Journal Name

ARTICLE TYPE

Cite this: DOI: 10.1039/xxxxxxxxxx

Water Plays a Dynamical Role in a Hydrogen-Bonded, Hexameric Supramolecular Assembly†

Ankita Katiyar,[a] Julia C. Freire Sovierzoski,[a] Paul B. Calio,[a‡] Anthony A. Vartia,[a] and Ward H. Thompson[a*]

Received Date
Accepted Date

DOI: 10.1039/xxxxxxxxxx

www.rsc.org/journalname

The hexameric resorcin[4]arene supramolecular assembly has attracted significant interest as a self-assembled capsule that exhibits dynamic host-guest chemistry. Many studies have been carried out to investigate the structure and thermodynamics of the assembly, but considerably less is known about its dynamical properties. Here, molecular dynamics simulations are used to investigate the timescales of water encapsulation in this assembly in wet chloroform. We have previously shown [*Chem. Commun.* **55**, 6591-6594 (2019)] that at low water content there are three distinct populations of water molecules present, while at higher water content an additional population, long water chains interacting with the assembly, appears. The relative free energies of these different water positions are calculated and time correlation functions are used to determine the timescales for interconversion between the populations. This analysis demonstrates that the water molecules are in rapid exchange with each other on timescales of tens of ps to a few ns, and suggests that water molecules might be acting as a critical component in the guest exchange mechanism.

1 Introduction

Self-assembled molecular containers have been known to the chemical community for decades and play a vital role in supramolecular chemistry.[1–8] These containers can be held together by different intermolecular interactions, among which hydrogen bonded (H-bonded) capsules have attracted significant attention.[9–17] Resorcin[4]arenes are a fascinating example of H-bonded self-assembled molecular capsules, which have been shown to accomodate a large range of guest molecules.[15–29]

The crystal structure of resorcin[4]arene hexamer, first reported by MacGillivray and Atwood,[30] shows that this hexameric assembly is an inflated cube with resorcin[4]arene monomers (Fig. 1) making up the six sides and a water molecule sitting at each of the eight corners. The assembly structure, which is held together by 60 H-bonds, is illustrated in Fig. 2. Each corner water molecule forms three hydrogen bonds; four water molecules donate two H-bonds and accept one, while the other four donate a single H-bond and accept two. The interior of the assembly is an octahedral-shaped cavity approximately ~ 1400 Å^3 in volume. Shivanyuk and Rebek showed that the resorcin[4]arene hexameric assembly forms in water-saturated $CDCl_3$ by encapsulating an alkylammonium guest molecule.[21] However, diffusion NMR studies demonstrated that guest molecules are not necessary for the formation of hexameric assembly.[31] Rather, the resorcin[4]arene hexameric assembly can self assemble by encapsulating solvent, *e.g.*, six $CDCl_3$ or eight benzene solvent molecules.[17–19,31–33]

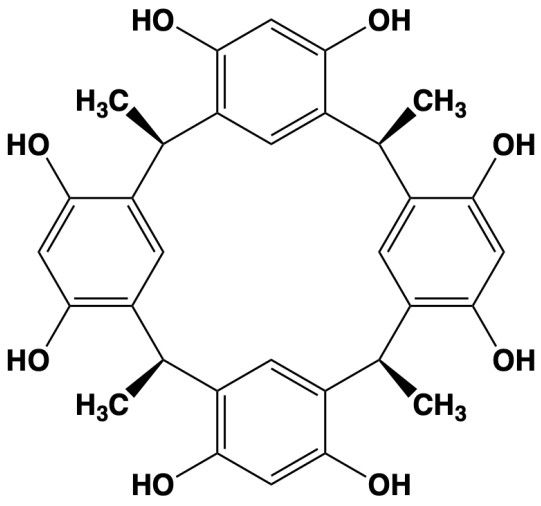

Fig. 1 Resorcin[4]arene monomer.

Hydrogen-bonded supramolecular assemblies create a barrier between the encapsulated guest molecules and the bulk solution

[a] *Department of Chemistry, University of Kansas, Lawrence, KS 66045, USA. E-mail: wthompson@ku.edu*
‡Current Address: Department of Chemistry, The University of Chicago, 5735 South Ellis Avenue, Chicago, Illinois 60637

such that guest encapsulation and release require the breaking of multiple H-bonds to form an opening. EXSY NMR spectroscopy has been used to determine the guest exchange rates and gain insight to the mechanisms[34] based on the shape and the size of the guest molecule for several H-bonded capsules.[35,36] For some capsules such as the calix[4]arene tetraurea dimer, guest exchange requires the complete dissociation of the assembly.[37] In other cases, like that of the glycoluril tetramer, only partial dissociation is observed during the guest exchange process.[38] For other capsules, such as Rebek's "tennis ball dimer,"[39] softballs,[40] and cylindrical assemblies[41] only some of the H-bonds are disrupted during guest exchange.[42,43]

The mechanisms of guest exchange are still unclear for the resorcin[4]arene hexameric assembly. A range of guest molecules, including several tetraalkylammonium salts, have been used to investigate the encapsulation process.[22,44] These studies suggest that the encapsulation of large tetraalkylammonium salts is entropically driven and it was posited that the guest exchange requires the complete dissociation of one resorcinarene monomer.[22] However, the steps and molecules involved in the process are still elusive.Other guest molecules like alcohols can form hydrogen bonds with the hexameric assembly and based on their size, are shown to coencapsulate with solvent molecules.[19] It has been shown that water molecules at the corner of the assembly can be replaced by suitable alcohol molecules.[24,45] Previous experimental studies indicate that for a range of capsules the optimal filling fraction is $\sim$ 55% of the host volume occupied by guest molecules,[46], though typically smaller values are observed for the resorcinarene assembly with results that depend upon the guest size and shape.[22,33] The water molecules are a crucial component of the hexameric resorcinarene capsule H-bonded framework and are required for the formation of the assembly. Their role in the stability of the assembly and in the guest exchange process, *e.g.*, as a lubricant that facilitates the assembly opening, is not well understood. Our focus on the behavior of the water molecules in the present work is motivated by this.

Understanding guest exchange for the hexameric resorcinarene capsule has been given greater impetus by several recent studies demonstrating its utility for hosting catalytic reactions.[47–62] Catalysis in the assembly requires reactant encapsulation and product release, either or both of which can slow the effective rate constant or turnover frequency. In addition, it has been reported that the water molecules in the assembly exhibit enhanced Brønsted acidity that can play a role in the catalysis.[52] A recent study has also found that the H-bonds donated by the water molecules can assist in catalysis.[48] Thus, the structure and dynamics of water molecules in and around the resorcinarene assembly has implications for understanding and designing such catalytic systems.

Recently, we have shown, using molecular dynamics (MD) simulations, that water molecules other than the eight that are part of the assembly structure interact with the assembly and there is a significant number of water molecules coencapsulated with the solvent molecules in the assembly. In the present work, we use MD simulations to provide new insight into the *dynamics* of the water molecules interacting with the resorcinarene hexameric assembly occurring on timescales that are too rapid to be accessed by NMR measurements.[13] The two main objectives of this work are to understand the dynamics of water molecules and how they are determined by the interactions between the excess water and the assembly. To our knowledge, this is the first MD study that quantitatively reports the free energies and dynamical timescales of water molecules in the resorcin[4]arene assembly in wet chloroform solvent.

2 Simulation Details

Classical MD simulations are carried out using the Large-scale Atomic/Molecular Massively Parallel Simulator (LAMMPS) software.[63,64] We used two simulation arrangements. In the first, one resorcin[4]arene hexameric supramolecular assembly is simulated with 8 to 16 water molecules in 2983 $CHCl_3$ solvent molecules in a cubic box of side length 73.05 Å. In the second, one resorcin[4]arene assembly was simulated with 40 and 50 water molecules in 7722 $CHCl_3$ molecules in a box of side length 103.525 Å. Both box sizes were selected to approximately match the experimental concentrations of water.[31,32] The SPC/E model is used to describe the water interactions while the General AMBER ForceField[65] (GAFF) was used for resorcinarene and chloroform.[66] Lennard-Jones and electrostatic interactions are evaluated with a cutoff of 12 Å. Long-range electrostatic interactions are included using three dimensional periodic boundary conditions and the damped-shifted force approach[67] with a damping parameter of $\alpha = 0.2$.

Thirteen trajectories are propagated for each system with a 1 fs time step and configurations saved every 100 fs. Each trajectory differed in the initial velocities, which are chosen randomly from a Boltzmann distribution. For each trajectory, the temperature is maintained for 5 ps using velocity rescaling followed by NVT propagation using a Nosé-Hoover thermostat[68,69] for a 0.725 ns equilibration period and finally a 15 ns data collection stage. Error bars are obtained using block averaging with each of the trajectories used as a block and are reported as 95% confidence intervals using the Student's t-distribution.[70]

3 Results

We have recently used the same MD simulation approach to identify as many as four distinct water populations in relation to the resorcin[4]arene hexameric assembly in wet chloroform.[71] These populations, which are illustrated in Fig. 2, can be differentiated based on the distance of the water molecule from the center-of-mass of the assembly (*vide infra*). Water molecules can be encapsulated within the assembly ("*encapsulated*"), represent part of the capsule structure through participation in the assembly H-bonding ("*structural*"), or be attached to the assembly *via* H-bonding with the eight structural water molecules ("*attached*"). Interestingly, other than the eight structural water molecules that are hydrogen bonded to the resorcinarene monomers, no significant H-bonding with the assembly monomers is observed. At low water content, monomer:water ratios of less than 6:16, water molecules found beyond 12.5 Å are found to be free in solution and uncoordinated to the assembly. However, at higher water content an additional ("*long chain*") population of water molecules in long H-bonded networks attached to the assembly

is found; hereinafter referred to as *long chain* water molecules. These are not necessarily linear chains but can be H-bonded clusters in a wide variety of arrangements.

In this paper, we further explore the thermodynamics of the water interactions with the resorcin[4]arene hexameric assembly as a function of water content in chloroform solvent (which is the most widely used solvent in studies of resorcin[4]arene hexameric assembly[13]) and make a first examination of the water exchange dynamics between the populations relative to the assembly. We note that the identity of the solvent almost surely affects the timescales and free energetics but there are no indications in the literature that changing the solvent to, for example, benzene fundamentally changes the assembly characteristics.[72]

3.1 Thermodynamics

To understand the thermodynamics of the water populations associated with the assembly, we calculated the (Helmholtz) free energy profile as a function of the total number of water molecules, N_{tot}, in the chloroform solution at 298 K. The free energy profiles are calculated as

$$\Delta A(r) = -RT \ln \left[\frac{P(r)}{P(r_0)} \right], \quad (1)$$

and the results from the simulations are shown in Fig. 3. Here, $\Delta A(r)$ is the free energy, R the gas constant, T the temperature, $P(r)$ the probability distribution as a function of the distance, r, between the centers-of-mass of a water molecule and the assembly, and r_0 a reference distance that defines the zero of energy. Note that $P(r)$ here includes the $4\pi r^2$ geometric factor accounting for the greater volume available to, *e.g.*, *attached* water molecules compared to *encapsulated* water molecules. In Fig. 3, the free energy minima can be identified for *encapsulated* water molecules ($r \simeq 5$ Å), *structural* water molecules (7–9 Å), and *attached* water molecules (~ 11 Å). At higher water content, $N_{tot} \geq 16$, an additional free energy minimum is observed in the range 13.5–15 Å, which corresponds to the *long chain* H-bonded water molecules. The structures corresponding to each of these minima are illustrated in Fig. 2.

The free energy profiles in Fig. 3 show that, not surprisingly, the most stable location for water molecules are the structural positions within the assembly. Indeed, we observe that eight structural water molecules are present at all times in our simulations for all water contents. We note that assembly does not dissociate, open, or exchange solvent molecule guests over the simulation time of nearly 0.2 microseconds per water content considered (~ 2 microseconds of total simulation time). This is consistent with the experimental reports that the assembly does not form in the absence of water. We note, however, that this result does not address whether the assembly is stable without water molecules. We carried out a long MD simulation of the pre-formed resorcinarene assembly in the complete absence of water (dry chloroform and all *structural* water molecules removed) and found it to be stable over a 100 ns simulation time. This indicates that the assembly is at least metastable without the presence of the *structural* water molecules.

The second most favorable location for water molecules is encapsulated within the assembly. The free energy of the encapsulated water molecules decreases rather quickly as excess water molecules are added and then little change is observed for $N_{tot} \geq 14$. The water molecules attached to the exterior of the capsule through H-bonding with the structural water molecules is the next most stable water arrangement. This free energy minimum also increases in stability with greater water content, but it continues to do so up to 50 total water molecules. The *long chain* structures only appear as a minimum for $N_{tot} \geq 16$ and are most prominent for 40 and 50 total water molecules. Thus, these arrangements are also favored at high water content.

The present results exhibit modest quantitative differences from our previous simulations reported in Ref. Katiyar *et al.*[71] because both the equilibration and collection stages are longer. We find that the total number of water molecules associated with the supramolecular assembly (total *encapsulated*, *attached*, and *long chain*) is 6.3 in water-saturated chloroform, is in good agreement with our analysis of NMR measurements that yields 6.0 water molecules.[32,71] These results are obtained by modeling the number of associated water molecules with an adsorption isotherm and, as we previously showed,[71] can be obtained by simulations or measurements of the water diffusion coefficient as a function of water content.

The free energy barriers to move between the populations are relatively modest. For the *structural* $\rightarrow$ *encapsulated* step illustrated in Fig. 2, the free energy barrier is $0.9-1.8$ kcal/mol, with the largest value occuring when only a single excess water is present ($N_{tot} = 9$). The *attached* $\rightarrow$ *structural* step has a free energy barrier of $\sim 0.8-1.2$ kcal/mol, but in this case the value is not clearly related to the water content. Larger effects are observed in the reverse process, *structural* $\rightarrow$ *attached* due to the greater stability of the *attached* structures with increasing N_{tot}. Thus, the barrier for this step is $\sim 1.7-3.5$ kcal/mol, decreasing as the total water content increases.

To further quantify how the free energy changes for moving between two populations a and b depends on the total water content, we calculated $\Delta A_{a\rightarrow b}$ for the two required steps of the encapsulation process *attached* $\rightarrow$ *structural* $\rightarrow$ *encapsulated* shown in Fig. 2. Each is calculated by integrating the probability distribution $P(r)$ over the range corresponding to the given population as defined by the dashed lines in Fig. 3, *e.g.*, between 6 and 10 Å for *structural* water molecules.

The results are provided in Fig. 4 and are well described by an adsorption isotherm model that is described in detail in the Appendix. As noted above, the *attached* $\rightarrow$ *structural* step is spontaneous ($\Delta A < 0$), but as the water content increases the *attached* state becomes relatively more stable and the magnitude of the free energy change decreases, plateauing at a value of -1.51 kcal/mol. The fitting to the adsorption isotherm model predicts the maximum number of *attached* water molecules to be 1.0; this corresponds to the $N_{tot} \rightarrow \infty$ limit and is thus representative of the water-saturated chloroform case. On the other hand, the *structural* $\rightarrow$ *encapsulated* step is not thermodynamically favored ($\Delta A > 0$). However, this step becomes less endergonic as the water content increases and the free energy change con-

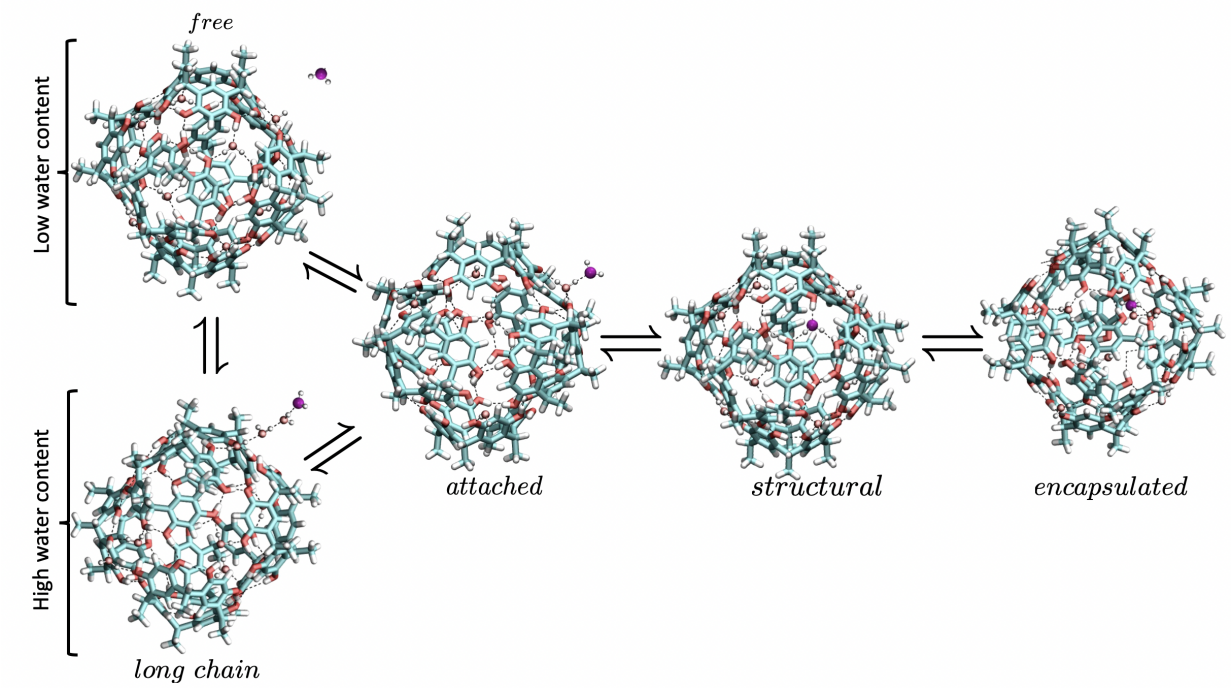

Fig. 2 The resorcin[4]arene hexameric assembly structure is shown along with water molecules in the five different populations identified, illustrated by the water molecules shown in purple. The *long chain* structures are only observed at higher water content (see the text). Color codes: carbon (cyan), oxygen (red), hydrogen (white), and H-bond (black dashed line).

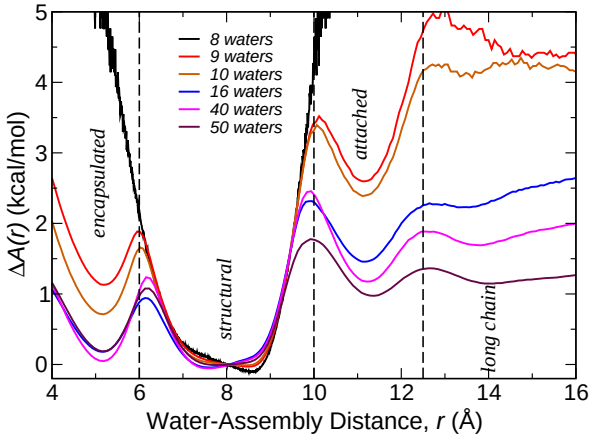

Fig. 3 Free energy profiles, $\Delta A(r)$, as a function of distance between the water and assembly centers-of-mass for different total number of water molecules, N_{tot}, in a solution with one hexameric assembly. The structures corresponding to the minima are illustrated in Fig. 2. Black dashed lines represent the dividing points between the different states.

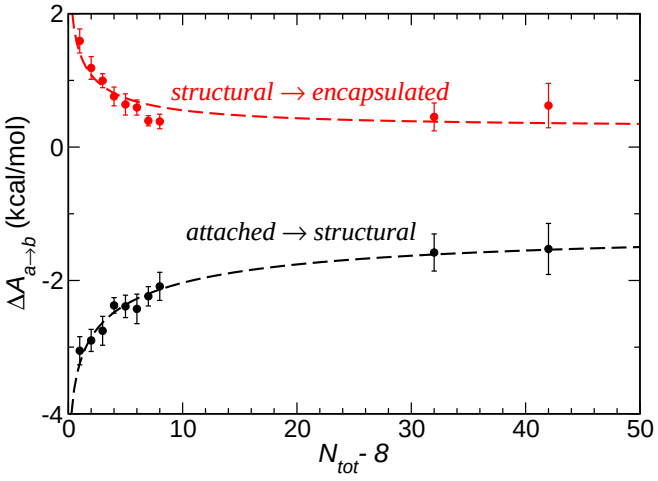

Fig. 4 Free energy change as a function of total water content (N_{tot}) between *structural* and *encapsulated* water molecules (red circles) and between *attached* and *structural* water molecules (black circles). Fits to the adsorption isotherm model detailed in the Appendix are also shown (dashed lines).

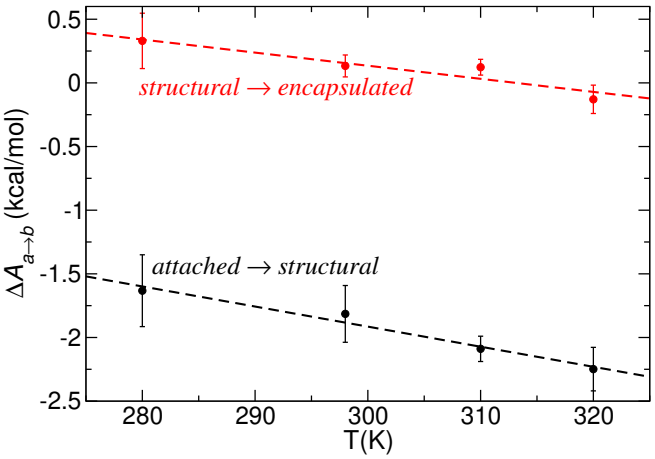

Fig. 5 Free energy change as a function of temperature is shown for the *attached* → *structural* step (black circles) and for the *structural* → *encapsulated* step (red circles) along with their linear fits (dashed lines).

verges to a value of 0.33 kcal/mol, which corresponds to a maximum number of 5.0 *encapsulated* water molecules. These limiting values for the free energy differences and maximum number of capsule-associated water molecules are those predicted for water-saturated chloroform (*i.e.*, large N_{tot}) based on the fitting of the data to the adsorption isotherm model.

The influence of temperature on the populations of water molecules interacting with the resorcinarene hexameric assembly can be used to determine the relative role of enthalpic and entropic effects. We therefore calculated the free energy change as a function of temperature for the 6:16 monomer:water ratio. This water content was selected because it is the highest water concentration in the smaller simulation box (making the calculations less computationally expensive) and it exhibits significant populations of *encapsulated* and *attached* waters. The results are shown in Fig. 5, where the free energy changes for the *attached* → *structural* and *structural* → *encapsulated* steps are plotted as a function of temperature. For both processes, $\Delta A_{a\to b}$ decreases as the temperature increases and is well fit by a line. The slope of the line is the change in entropy, $\Delta S_{a\to b}$, since

$$\Delta A_{a\to b} = \Delta U_{a\to b} - T\Delta S_{a\to b} \qquad (2)$$

The change in internal energy, $\Delta U_{a\to b}$ at 298 K is obtained by solving Eq. 2 given the calculated free energy and entropy changes. The values for the free energy, internal energy, and entropy changes are given in Table 1.

This van't Hoff analysis reveals that both steps are endothermic and also are associated with positive entropy changes. The $\Delta S_{a\to b}$ associated with the *attached* → *structural* step is larger, by ∼ 40%, than that for the *structural* → *encapsulated* process, but this difference is not significant outside the error bars. It is somewhat surprising that the entropy change for the *attached* → *structural* step is both positive and significantly so. This result is the opposite of what would be expected based only on the geometric factors, *i.e.*, the volume occupied by the *attached* water molecules is nominally larger than that for the *structural* water molecules. Moreover, the *structural* water molecules would appear to be more constrained in the configurations they can adopt as part of the assembly structure. However, there are two features that can be used to understand this result. First, note that the assembly structure, while robust, is quite flexible, which can be seen in the broad free energy minimum corresponding to *structural* water molecules shown in Fig. 3. In comparison, the minimum corresponding to *attached* water molecules is quite narrow. Second, the *attached* water molecules are bound to a *structural* water, either as an H-bond donor or acceptor, or H-bonded to other *attached* water molecules. This significantly reduces the number of conformations that are available to the *attached* water molecules.

The same two features can be used to understand the entropy change in *structural* → *encapsulated* step and would suggest it should have a negative entropy, in contrast to the results in Table 1. The difference appears to be the larger number of *encapsulated* water molecules, more than twice that of *attached* water molecules,[71] which increases the relative entropy. That is, the larger entropy of the *encapsulated* water molecules is associated with the greater number of arrangements the molecules can adopt because there are multiple *encapsulated* water molecules.

3.2 Dynamics

The water molecules in different populations illustrated in Fig. 2 exchange with each other by breaking and forming H-bonds, but the associated rate constants have not been determined experimentally because the exchange is fast on the NMR timescale.[31,32] Here we address this issue by quantitatively characterizing the exchange dynamics using MD simulations. Specifically, we calculate time correlation functions (TCFs) associated with water molecule exchange between two states, which give access to the associated rate constants as described below.

Consistent with our analysis of the free energy curves, we determine the state of a given water molecule based on the four radial dividing surfaces defined in terms of the distance to the assembly center-of-mass. These are located at $r = 6$, 10, 12.5, and 16 Å and indicated in Fig. 3. Then for the transition of a water molecule from state a to state b, we calculate the TCF,[73]

$$C_{a\to b}(t) = \langle h_a(0)\, h_b(t)\rangle\,. \qquad (3)$$

Here, the $h_x(t)$ function is one (zero) for a water molecule that is (is not) in state x at time t. Thus, $C_{a\to b}(0) = 0$ but rises with time as molecules that are initially in state a ($h_a(0) = 1$; $h_b(0) = 0$) transition to state b ($h_b(t) = 1$). For a simple rate process, the rise is exponential in time governed by the rate constant $k_{a\to b}$. The TCF is obtained by averaging, indicated by the brackets $\langle\cdot\rangle$, over the different possible choices of the initial time, $t = 0$, throughout the MD trajectory as well as the different water molecules. Absorbing boundary conditions are used so that once a water molecule has changed states, $h_b(t)$ is taken as 1 for all times thereafter; in this way the TCF only contains information about the forward process, $a \to b$.

Table 1 Thermodynamics of water encapsulation at 298 K for $N_{tot} = 16$: Calculated free energy ($\Delta A_{a\to b}$), internal energy ($\Delta U_{a\to b}$), entropy ($\Delta S_{a\to b}$), and entropic contribution ($T\Delta S_{a\to b}$); units are kcal/mol except for entropy which is in cal/(mol · K). Subscripts indicate the uncertainties in the final digit(s). *adsorbed* population is a combined population of *attached* and *encapsulated*.

$a \to b$	$\Delta A_{a\to b}$	$\Delta U_{a\to b}$	$\Delta S_{a\to b}$	$T\Delta S_{a\to b}$
attached → *structural*	-2.1_2	2.1_9	$14.1_{3.0}$	4.2_9
structural → *encapsulated*	0.4_1	$3.6_{1.5}$	$10.7_{5.0}$	$3.2_{1.5}$
free → *adsorbed*	-0.9_2	$2.3_{1.0}$	$10.7_{3.4}$	$3.2_{1.0}$

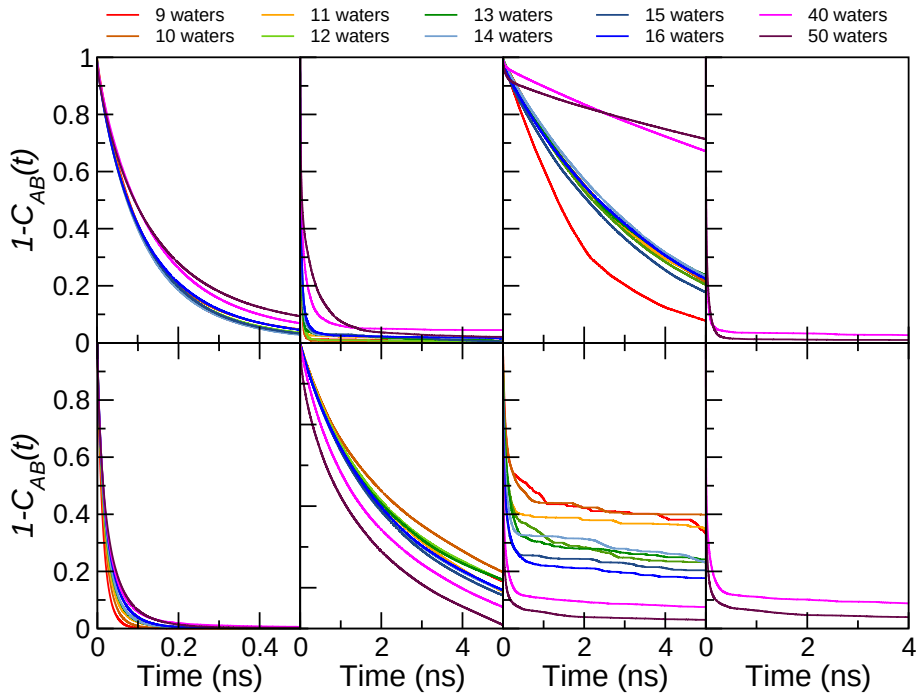

Fig. 6 Time correlation functions, $C_{a\to b}(t)$, are plotted versus time for different water content, $N_{tot} = 9-50$. The first (second) row shows from left to right the TCFs for the forward (backward) processes illustrated in Fig. 2.

The sequential nature of the water exchange processes illustrated in Fig. 2 gives rise to three (four) steps that a water free in solution must undergo to be encapsulated in the assembly at low (high) water content. Each of these has a corresponding reverse step. The TCFs for these eight exchange processes are plotted in Fig. 6. The nature of the kinetics differs between steps: some of the processes are single exponential and hence characterized by a single rate constant such that

$$1 - C_{a\to b}(t) \cong A_{a\to b}\, e^{-k_{a\to b}t}. \qquad (4)$$

Others are bi-exponential and several can only be fit by including an offset, *e.g.*,

$$1 - C_{a\to b}(t) \cong A_f\, e^{-k^f_{a\to b}t} + A_s\, e^{-k^s_{a\to b}t} + (1 - A_f - A_s), \qquad (5)$$

where "f" and "s" indicate the faster and slower rate constants. Here, $(1 - A_f - A_s)$ represents the offset that corresponds to a process occurring on a longer timescale than can be accessed in the simulations.

Some of the complexity of the kinetics arises from the conditions that must be in place for particular processes. For example, for the *structural* → *attached* step to take place an *encapsulated* water molecule must be H-bonded to the *structural* water, else the process would leave the assembly without a *structural* water, something that is not observed in the simulations and hence strongly disfavored. This requirement leads to a significant offset in describing the *structural* → *attached* TCF. Similar arguments can be made for other steps represented in Fig. 6 that require some pre-arrangement.

We begin by considering the *structural* ⇌ *encapsulated* step. The *encapsulated* water molecules convert rapidly to structural water molecules, with a time constant of $\tau_{a\to b} = k^{-1}_{a\to b} \simeq 20$ ps. The forward process is slower, as anticipated from its endergonicity indicated in Fig. 3, and bi-exponential with time scales of 60

and 190 ps and a small offset (< 5%); it is the longer timescale that represents the dominant component. The dynamics of both processes are relatively independent of the water content, with the primary effect observed for $N_{tot} = 9$, for which the forward step is faster and the reverse step is slower.

Next, we consider the *attached* ⇌ *structural* step. The forward step is best described by a bi-exponential fit with a fast time scale of few ps and a slow time scale of ∼ 40 ps at low water content, whereas, at high water content, the process becomes even slower and gives a slow time scale of ∼ 300 ps. This agrees with the free energy diagram in Fig. 3, which shows that as the water content increases, the barrier to go from *attached* to *structural* increases. This result suggests that the water exchange within the long chain that is interacting with the structural water may slow down this process. The reverse step *structural* ⇌ *attached* is similarly best described by a bi-exponential fit with a dominating slow time scale of ∼ 5-6 ns at low water content and ∼ 2-3 ns at high water content. This is also consistent with the results presented in Fig. 3, which show the barrier decreasing with N_{tot}.

Both the forward and reverse steps for the*free* ⇌ *attached* process are described by a bi-exponential fit, except for the forward step with $N_{tot} = 9$, which exhibits a single exponential decay with a ∼ 2 ns time scale. The forward process is slower, indicating *free* water molecules in the solution require significant time to find a *structural* water. The dynamics of the forward step changes from ∼ 3 ns at low water content to ∼ 15 ns for 40 or 50 total water molecules. The reverse process occurs on a fast timescale of 60 ps and a slow one of 3-4 ns at low water content, which are reduced to 10 ps and 500 ps, respectively at high water content. The *attached* → *free* water dynamics further changes its behavior as the water content is changed: at low water content the slow time scale has the larger amplitude but as N_{tot} increases the fast timescale becomes the dominant component. This trend suggests that the formation of a *long chain* structure may facilitate this reverse step, *e.g.*, by stabilizing the nascent *free* water when it breaks the H-bond with a *structural* water.

At high water content ($N_{tot} = 40$ and 50), there is an additional step of *long chain* ⇌ *attached*, which has a slow time scale of ∼ 60 ps and a fast timescale of ∼ 5 ps. The backward step is slower with timescales of ∼ 300 ps and 8 ps. The fast timescale is the dominant component in both the forward and reverse step. This suggests that the long chains are transient and there is fast exchange among the water molecules within the H-bonded network.

A schematic illustration of the free energies of the different water populations associated with the assembly and the timescales for exchange between them is shown in Fig. 7 for the limiting cases of 9 and 50 water molecules. A smoothed free energy profile is presented for each, obtained by interpolating the calculated free energy shown in Fig. 3. To provide a complete picture of the water dynamics relative to the resorcinarene assembly for these limiting cases, approximate timescales for the transitions of water molecules between populations are given next to the free energy barrier associated with the process. The values shown are those associated with the dominant component of the dynamics in each case. Not shown in Fig. 7 are the timescales for transitions between *free* and *attached* water molecules.

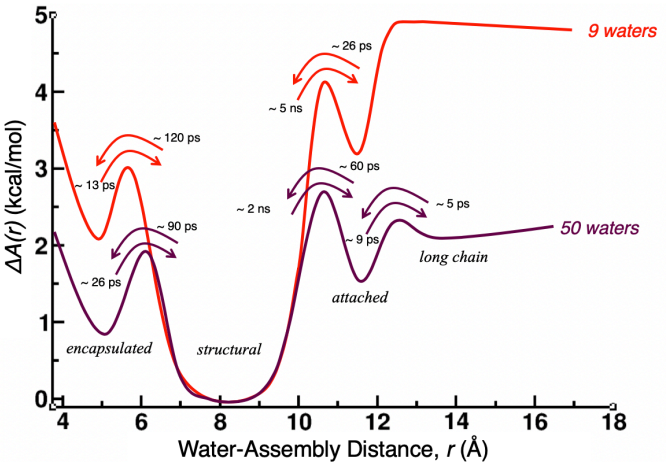

Fig. 7 Schematic of the free energy surface and timescales for 9 (red) and 50 (aubergine) total water molecules.

4 Conclusions

In this study, the thermodynamic and dynamical properties of resorcin[4]arene hexameric supramolecular assemblies in wet chloroform were investigated using MD simulations. The results show that the eight *structural* water molecules, which are part of the assembly framework, are the most stable. In fact, the simulations do not observe any absence of these water molecules in any of the simulations over the full range of water content. The association of other water molecules with the assembly occurs with three motifs: *i) encapsulated* within, *ii) attached* through H-bonding to the *structural* water molecules, or *iii)* in a transient H-bonded *long chain* of water molecules, in order of decreasing stability. Each of these water populations becomes more favorable as the solution water content is increased, with the *long chain* water molecules appearing only at higher water content. Moreover, a van't Hoff analysis demonstrates that the free energy surface is strongly affected by entropic contributions that may, at first glance, appear counterintuitive.

We have also investigated the timescales of the water exchange between different populations associated with the resorcinarene capsule. The slowest dynamics is observed for free water molecules in solution to become *attached* through H-bonding to the *structural* water molecules in the assembly. This step is found to occur on the timescale of $3-15$ ns (depending on the water content of the solution) consistent with prior reports that water exchange is rapid on the NMR timescale.[31,32]

The other water exchange processes span a wide range of timescales from picoseconds to nanoseconds. The more thermodynamically favorable steps, *e.g.*, *encapsulated* → *structural* or *attached* ⇌ *long chain*, are rapid, taking place in only $\sim 5-10$ ps. On the other hand, the endergonic exchanges, primarily those originating with the stable *structural* water molecules, occur on timescales ranging from approximately 100 ps to a few ns.

The results presented here represent predictions for the dy-

namical timescale of water around the resorcinarene assembly as, to our knowledge, there are currently no measurements of these processes. It is hoped that these simulations can inspire the application of additional experimental techniques that will shed new light on the capsule dynamics.

The rich dynamics is reflective of the underlying free energy for water molecules as a function of position relative to the assembly and representative of the interesting and important role water plays in the properties of the assembly. The persistent nature of the water molecules associated with the resorcinarene hexameric capsule[32,71] and the facile transitions between different arrangements relative to the assembly raise important questions. Foremost among these are: Are these water molecules involved in the process of guest exchange? Do they serve to stabilize the broken H-bonds of the assembly when it opens to permit guest encapsulation or release? Do the dynamics of the water H-bonding patterns play a role in determining the timescales for guest exchange?

The present results thus point to the importance of considering the involvement of water molecules in larger scale resorcinarene assembly dynamics such as guest exchange or monomer dissociation. The mechanisms of these processes are still not understood and are critical areas for future simulation studies.

Conflicts of interest

There are no conflicts to declare.

Acknowledgments

The authors thank Pubudu N. Wimalasiri for many useful discussions. This work was supported by the American Chemical Society Petroleum Research Fund (Grant #57419-ND6). The authors gratefully acknowledge CAPES for a scholarship granted to J.C.F.S and support from the NSF-REU program for P.B.C. (CHE-1263259) and J.C.F.S. (CHE-1560279). The calculations were performed at the University of Kansas Center for Research Computing (CRC).

Appendix

We previously showed that the number of water molecules bound (*encapsulated*, *attached*, and *long chain* molecules) to the resorcinarene hexameric assembly can be described by a simple adsorption isotherm.[71] Applying this to the *encapsulated* blackwater molecules alone gives

$$N_{enc} = \frac{K_{enc}(N_{tot}-8)}{1+K_{enc}(N_{tot}-8)} N_{enc}^{max}, \qquad (6)$$

where N_{enc}^{max} is the maximum number of *encapsulated* water molecules obtained at larger N_{tot} (*i.e.*, in water-saturated chloroform) and K_{enc} is an effective equilibrium constant. The total number of water molecules used in this expression is $N_{tot}-8$ based on the assumption (validated in the simulations) that eight *structural* water molecules are always present and thus not available for encapsulation (without being replaced). Within a constant shift, the free energy difference for the *structural* $\rightarrow$ *encapsulated* transition is given by

$$\Delta A_{str\rightarrow enc} = -RT \ln\left[\frac{N_{enc}}{N_{str}}\right] = -RT \ln\left[\frac{N_{enc}}{8}\right], \qquad (7)$$

using the fact that $N_{str} = 8$. Combining this with Eq. 6 gives

$$\Delta A_{str\rightarrow enc} = -RT \ln\left[\frac{K_{enc}(N_{tot}-8)}{1+K_{enc}(N_{tot}-8)} \frac{N_{enc}^{max}}{8}\right]. \qquad (8)$$

This is the adsorption isotherm description used to fit the results presented in Fig. 2 for the *structural* $\rightarrow$ *encapsulated* free energy. An analogous expression that differs by the leading negative sign is used for the *attached* $\rightarrow$ *structural* result.

References

1 M. Fujita, K. Umemoto, M. Yoshizawa, N. Fujita, T. Kusukawa and K. Biradha, *Chem. Commun.*, 2001, 509–518.
2 Y. Inokuma, M. Kawano and M. Fujita, *Nat. Chem.*, 2011, **3**, 349.
3 T. S. Koblenz, J. Wassenaar and J. N. Reek, *Chem. Soc. Rev.*, 2008, **37**, 247–262.
4 M. D. Pluth, R. G. Bergman and K. N. Raymond, *Acc. Chem. Res.*, 2009, **42**, 1650–1659.
5 J. Meeuwissen and J. N. Reek, *Nat. Chem.*, 2010, **2**, 615.
6 D. Ajami and J. Rebek Jr., *Acc. Chem. Res*, 2013, **46**, 990–999.
7 M. Raynal, P. Ballester, A. Vidal-Ferran and P. W. Van Leeuwen, *Chem. Soc. Rev.*, 2014, **43**, 1734–1787.
8 S. Zarra, D. M. Wood, D. A. Roberts and J. R. Nitschke, *Chem. Soc. Rev.*, 2015, **44**, 419–432.
9 F. Hof, S. L. Craig, C. Nuckolls and J. Rebek, Jr, *Angew. Chem. Intl. Ed.*, 2002, **41**, 1488–1508.
10 S. M. Biros and J. Rebek Jr, *Chem. Soc. Rev.*, 2007, **36**, 93–104.
11 O. B. Berryman, H. Dube and J. Rebek Jr, *Isr. J. Chem.*, 2011, **51**, 700–709.
12 K.-D. Zhang, D. Ajami and J. Rebek, *J. Am. Chem. Soc.*, 2013, **135**, 18064–18066.
13 L. Avram and Y. Cohen, *Chem. Soc. Rev.*, 2015, **44**, 586–602.
14 T. Adachi and M. D. Ward, *Acc. Chem. Res.*, 2016, **49**, 2669–2679.
15 C. Gaeta, C. Talotta, M. De Rosa, P. La Manna, A. Soriente and P. Neri, *Chem. Eur. J.*, 2019, **25**, 4899–4913.
16 J. Rebek Jr, *Angew. Chem.Intl. Ed.*, 2005, **44**, 2068–2078.
17 L. Avram, Y. Cohen and J. Rebek Jr., *Chem. Commun.*, 2011, **47**, 5368–5375.
18 L. Avram and Y. Cohen, *J. Am. Chem. Soc.*, 2004, **126**, 11556–11563.
19 T. Evan-Salem, I. Baruch, L. Avram, Y. Cohen, L. C. Palmer and J. Rebek, *Proc. Natl. Acad. Sci.*, 2006, **103**, 12296–12300.
20 L. Avram and Y. Cohen, *J. Am. Chem. Soc.*, 2003, **125**, 16180–16181.
21 A. Shivanyuk and J. Rebek, *Proc. Natl. Acad. Sci.*, 2001, **98**, 7662–7665.
22 M. Yamanaka, A. Shivanyuk and J. Rebek, *J. Am. Chem. Soc.*, 2004, **126**, 2939–2943.
23 L. Avram and Y. Cohen, *Org. Lett.*, 2008, **10**, 1505–1508.

24 O. Ugono and K. T. Holman, *Chem. Commun.*, 2006, 2144–2146.

25 S. Slovak, L. Avram and Y. Cohen, *Angew. Chem. Intl. Ed.*, 2009, **49**, 428–431.

26 Y. Qiu and A. E. Kaifer, *Isr. J. Chem.*, 2011, **51**, 830–839.

27 S. Yi, E. Mileo and A. E. Kaifer, *Org. Lett.*, 2009, **11**, 5690–5693.

28 E. Mileo, S. Yi, P. Bhattacharya and A. E. Kaifer, *Angew. Chem. Intl. Ed.*, 2009, **48**, 5337–5340.

29 I. E. Philip and A. E. Kaifer, *J. Am. Chem. Soc.*, 2002, **124**, 12678–12679.

30 L. R. MacGillivray and J. L. Atwood, *Nature*, 1997, **389**, 469–472.

31 L. Avram and Y. Cohen, *J. Am. Chem. Soc.*, 2002, **124**, 15148–15149.

32 L. Avram and Y. Cohen, *Org. Lett.*, 2002, **4**, 4365–4368.

33 A. Shivanyuk and J. Rebek, *J. Am. Chem. Soc.*, 2003, **125**, 3432–3433.

34 K. Nikitin and R. O'Gara, *Chem. Eur. J.*, 2019, **25**, 4551–4589.

35 L. C. Palmer, A. Shivanyuk, M. Yamanaka and J. Rebek Jr, *Chem. Commun.*, 2005, 857–858.

36 M. D. Pluth and K. N. Raymond, *Chem. Soc. Rev.*, 2007, **36**, 161–171.

37 O. Mogck, M. Pons, V. Böhmer and W. Vogt, *J. Am. Chem. Soc.*, 1997, **119**, 5706–5712.

38 F. Hof, C. Nuckolls, S. L. Craig, T. Martín and J. Rebek, *J. Am. Chem. Soc.*, 2000, **122**, 10991–10996.

39 T. Szabo, G. Hilmersson and J. Rebek, *J. Am. Chem. Soc.*, 1998, **120**, 6193–6194.

40 J. Santamaría, T. Martín, G. Hilmersson, S. L. Craig and J. Rebek, *Proc. Natl. Acad. Sci.*, 1999, **96**, 8344–8347.

41 S. L. Craig, S. Lin, J. Chen and J. Rebek, *J. Am. Chem. Soc.*, 2002, **124**, 8780–8781.

42 T. Szabo, G. Hilmersson and J. Rebek, *J. Am. Chem. Soc.*, 1998, **120**, 6193–6194.

43 L. C. Palmer and J. Rebek Jr, *Org. Biomol. Chem.*, 2004, **2**, 3051–3059.

44 S. Slovak and Y. Cohen, *Supramol. Chem.*, 2010, **22**, 803–807.

45 S. Slovak and Y. Cohen, *Chem. Eur. J.*, 2012, **18**, 8515–8520.

46 S. Mecozzi and J. Rebek, Jr, *Chem. Eur. J.*, 1998, **4**, 1016–1022.

47 C. Gaeta, C. Talotta, M. De Rosa, P. La Manna, A. Soriente and P. Neri, *Chem. Eur. J.*, 2019, **25**, 4899–4913.

48 P. La Manna, C. Talotta, G. Floresta, M. De Rosa, A. Soriente, A. Rescifina, C. Gaeta and P. Neri, *Angew. Chem. Intl. Ed.*, 2018, **57**, 5423–5428.

49 A. Cavarzan, A. Scarso, P. Sgarbossa, G. Strukul and J. N. Reek, *J. Am. Chem. Soc.*, 2011, **133**, 2848–2851.

50 A. Cavarzan, J. N. Reek, F. Trentin, A. Scarso and G. Strukul, *Catal. Sci. Technol.*, 2013, **3**, 2898–2901.

51 G. La Sorella, L. Sperni, P. Ballester, G. Strukul and A. Scarso, *Catal. Sci. Technol.*, 2016, **6**, 6031–6036.

52 Q. Zhang and K. Tiefenbacher, *J. Am. Chem. Soc.*, 2013, **135**, 16213–16219.

53 Q. Zhang and K. Tiefenbacher, *Nat. Chem.*, 2015, **7**, 197 –202.

54 L. Catti and K. Tiefenbacher, *Chem. Commun.*, 2015, **51**, 892–894.

55 L. Catti and K. Tiefenbacher, *Chem. Commun.*, 2014, **51**, 892–894.

56 T. M. Bräuer, Q. Zhang and K. Tiefenbacher, *Angew. Chem. Intl. Ed.*, 2016, **128**, 7829–7832.

57 L. Catti, Q. Zhang and K. Tiefenbacher, *Synthesis*, 2016, **48**, 313–328.

58 Q. Zhang, L. Catti, J. Pleiss and K. Tiefenbacher, *J. Am. Chem. Soc.*, 2017, **139**, 11482–11492.

59 L. Catti, A. Pöthig and K. Tiefenbacher, *Adv. Synth. Catal.*, 2017, **359**, 1331–1338.

60 L. Catti and K. Tiefenbacher, *Angew. Chem. Intl. Ed.*, 2018, **57**, 14589–14592.

61 Q. Zhang, L. Catti and K. Tiefenbacher, *Acc. Chem. Res*, 2018, **51**, 2107–2114.

62 Q. Zhang and K. Tiefenbacher, *Angew. Chem. Intl. Ed.*, 2019, **58**, 12688–12695.

63 S. Plimpton, *J. Comput. Phys.*, 1995, **117**, 1–19.

64 The LAMMPS molecular dynamics package, http://lammps.sandia.gov.

65 J. Wang, R. M. Wolf, J. W. Caldwell, P. A. Kollman and D. A. Case, *J. Comp. Chem.*, 2004, **25**, 1157–1174.

66 H. J. C. Berendsen, J. R. Grigera and T. P. Straatsma, *J. Phys. Chem.*, 1987, **91**, 6269–6271.

67 C. J. Fennell and J. D. Gezelter, *J. Chem. Phys.*, 2006, **124**, 234104.

68 S. Nosé, *Mol. Phys.*, 1984, **52**, 255–268.

69 W. G. Hoover, *Phys. Rev. A*, 1985, **31**, 1695–1697.

70 D. P. Shoemaker, C. W. Garland and J. Nibler, *Experiments in Physical Chemistry*, McGraw-Hill: New York, 1989.

71 A. Katiyar, J. C. F. Sovierzoski, P. B. Calio, A. A. Vartia and W. H. Thompson, *Chem. Commun.*, 2019, **55**, 6591–6594.

72 L. Avram and Y. Cohen, *Org. Lett.*, 2006, **8**, 219–222.

73 S. H. Northrup and J. T. Hynes, *J. Chem. Phys.*, 1980, **73**, 2700–2714.

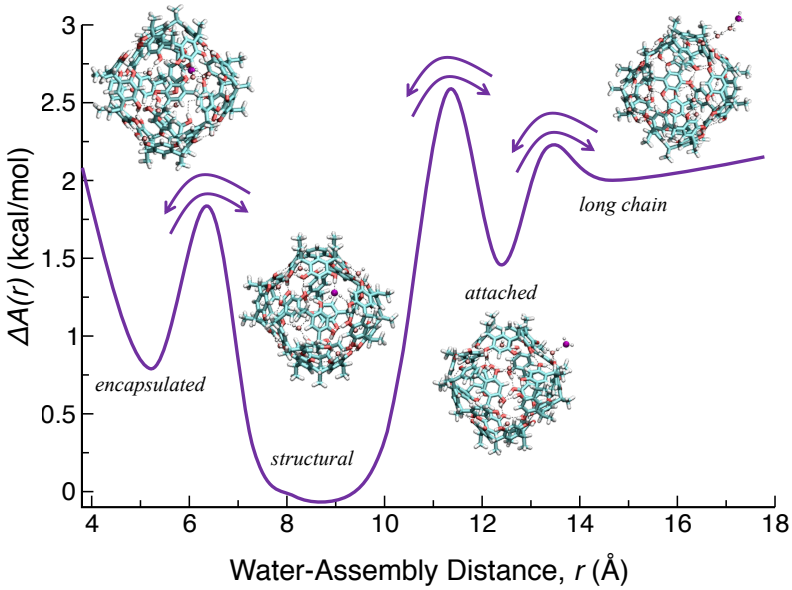

Water molecules associated with a hexameric resorcin[4]arene supramolecular assembly exchange on timescales from picoseconds to nanoseconds